N O T I C E

THIS DOCUMENT HAS BEEN REPRODUCED FROM MICROFICHE. ALTHOUGH IT IS RECOGNIZED THAT CERTAIN PORTIONS ARE ILLEGIBLE, IT IS BEING RELEASED IN THE INTEREST OF MAKING AVAILABLE AS MUCH INFORMATION AS POSSIBLE

NASA TECHNICAL MEMORANDUM NASA TM 75921

NUMERICAL MODELING OF STIMULATION OF INDUCED MAGNETOSPHERE DURING INTERACTION OF SOLAR WIND WITH THE IONOSPHERE OF VENUS

A. S. Lipatov

Translation of: "Chislennoye modelirovaniye vozbuzhdeniya indutsirovannoy magnitosfery pri vzaimodeystvii solnechnogo vetra s ionosferoy venery," USSR Academy of Sciences, Institute of Cosmic Research, Preprint No. 351, Moscow, 1977, pp 1-24

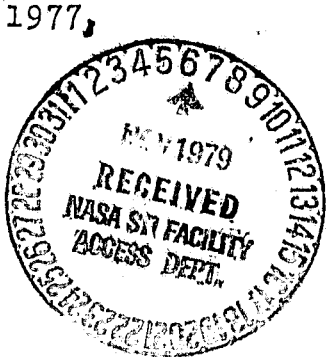

NATIONAL AERONAUTICS AND SPACE ADMINISTRATION
Washington, D. C. October 1979

TABLE OF CONTENTS

INTRODUCTION		1
I.	MATHEMATICAL FORMULATION OF THE PROBLEM. Solar wind model. Ionosphere model. Initial and boundary conditions.	2
II.	NUMERICAL MODELING METHOD Discrete model of plasma. Differential method of solving Maxwell's equations.	5
III.	RESULTS OF CALCULATIONS	7
CONCLUSIONS		9
REFERENCES		11
FIGURE CAPTIONS		13

NUMERICAL MODELING OF STIMULATION OF INDUCED MAGNETOSPHERE DURING INTERACTION OF SOLAR WIND WITH THE IONOSPHERE OF VENUS

A. S. Lipatov

INTRODUCTION

/3*

Measurements of plasma and magnetic field in the vicinity of Mars [1-4] and Venus [4-6] have discerned a "head" non-colliding shock wave, a weak magnetic force on Mars ~ 50 γ and the absence of a field on the surface of Venus.

At the present time, gasdynamic models of atmospheric flow of Mars and Venus [7-8] are known. It has been supposed that the external boundary of the atmosphere is a tangential break, and the braking pressure in the transitional sphere is balanced by the pressure of the atmosphere.

Also known are quasi-hydrodynamic evaluations of the value of induced magnetic field associated with the diamagnetism of photoions and conductivity of the ionosphere, which do not consider reverse influence of the field on flow in the transitional sphere [9].

Direct numerical modeling of the interaction of solar wind plasma with the ionosphere [10] has shown that in the case of subsonic flow, an induced magnetosphere may exist. However, further calculations on supersonic regimes have shown that plasma and solar wind currents are locked on the ionosphere.

---

*Numbers in margin indicate pagination of original foreign text.

This fact has led to the necessity of considering interaction processes in the ionopause in the overall flow diagram.

This work is devoted to the study of:

1) electrodynamic processes in the ionopause;
2) the structure of the induced magnetosphere.

MATHEMATICAL FORMULATION OF THE PROBLEM

/4

Solar wind model. Proceeding from solar wind conditions

$$\tau_e \ll \delta_u \sim \tau_i \,, \quad \omega_e \gg \frac{D}{Dt} \ln H$$

we will describe electrons by equations of magnetic hydrodynamics, and ions by function of distribution in a dimensionless form:

generalized Ohm's law

$$\vec{E} = -\vec{W} \times \vec{H} + \frac{W_\infty}{\omega_i R^* n}\left(\frac{1}{M_a^2}\operatorname{rot}\vec{H}\times\vec{H} - \frac{\nabla P_e}{\varkappa M_3^2}\right) + \frac{\operatorname{rot}\vec{H}}{Re_m} \,; \tag{1}$$

equation of condition for electron component

$$P = n^{\varkappa} \,; \tag{2}$$

equation for ions

$$\left(\frac{\partial}{\partial t} + \vec{V}_i \nabla_r + \dot{\vec{V}}_i \nabla_V\right) f = 0 \,, \tag{3}$$

$$\frac{D}{Dt}\vec{V}_i = \frac{\omega_i R^*}{W_\infty}\left(\vec{E} + \vec{V}_i \times \vec{H}\right) \,;$$

Maxwell's induction equation

$$\frac{\partial}{\partial t}\vec{H} = -\operatorname{rot}\vec{E}, \qquad (4)$$

where $\vec{W} = \langle \vec{V}_i \rangle$ -- average macroscopic speed of plasms, M_a , M_s -- alvenous and sonic Mach numbers, W_∞ , ω_i -- unstimulated speed of solar wind and ion gyrofrequency, R* -- characteristic dimension of the problem -- outside radius of the ionosphere, $R_{em} = \frac{4\pi W_\infty R^* \sigma}{c^2}$ -- Reynold's magnetic number, $\varkappa$ -- effective adiabatic indicator (in computations $\varkappa = 5/3$), σ -- conductivity. /5

The transition from dimensional variables to dimensionless is determined by formulas:

$$t = \frac{R^*}{W_\infty} t' ; \quad r = R^* r' ; \quad W = W_\infty W' ;$$

$$n = n_\infty n' ; \quad H = H_\infty H' ;$$

$$E = \frac{W_\infty H_\infty}{c} E' ; \quad P = P_\infty P'$$

Ionosphere model. Let us suppose that the parameters of the planet's atmosphere are known. Then the dynamics of the ionosphere is described by equations of motion, field, and indissolubility:

$$\frac{D}{Dt}\vec{V}_u = -\frac{\operatorname{rot}\vec{H}\times\vec{H}}{M_a^2 n_u \bar{M}_u} - \frac{\nabla P_u}{\varkappa M_s n_u} + \frac{R^*}{M W_\infty^2}\vec{F}_{TP} ; \qquad (5)$$

$$\vec{E} = -\frac{n_u\vec{V}_u + n\vec{W}}{n_u} + \frac{W_\infty}{\omega_i R^*}\frac{\operatorname{rot}\vec{H}\times\vec{H}}{M_a^2 n_u} + \frac{\operatorname{rot}\vec{H}}{Re_{mu}} - \qquad (6)$$

$$- \frac{\nabla P_u}{\varkappa M_3^2 n_u} \cdot \frac{W_\infty}{\omega_i R^*} - \frac{\vec{F}_{TP}}{M W_\infty \omega_i} ; \quad (7)$$

$$\frac{\partial \vec{H}}{\partial t} = - rot \vec{E} ; \quad (8)$$

$$\frac{D}{Dt} n_u = \frac{R^*}{W_\infty} \alpha n_n - \frac{R^* n_\infty}{W_\infty} \gamma n_u^2 ;$$

n_u, n_n -- concentration of charged and neutral particles,
α, γ -- coefficients of photoionization and recombination,
V_u, P_u -- speed and pressure in the ionosphere,
F_{TP} -- force of friction with neutral particles.

The presented mathematical model of the ionosphere is rather complex. Since in this work we are primarily interested in processes in the transitional sphere and in the ionopause, we will examine a simplified model of the ionosphere: 16

1) The distribution of charged particles in the ionosphere is stationary;

2) convection in the ionosphere in the first approximation is absent $\vec{V_u} = 0$;

3) "throw-off" of magnetic field from the ionosphere is determined by effective conductivity

$$R_{eHu} = 10^1 \div 10^5 < R_{eH}^* \quad (R_{em}^*$$

-- Reynolds number determined by Coulomb collisions);

4) the ionosphere has the form of a spherical ring with thickness δ_u .

Initial and boundary conditions. It is assumed that at an initial moment in time, the ionosphere is submerged in a homogeneous interplanetary magnetic field. The parameters of plasma

in the vicinity of the ionosphere are also unstimulated. At the outside boundary of the computed sphere (half the spherical ring, Fig. 1) $R = R_K$, parameters of the oncoming plasma flow and fields correspond to interplanetary, and $\vec{W}_\infty \perp \vec{H}_\infty$. At the boundary sphere $\theta = \pi/2$, homogeneous boundary conditions of type II $\frac{\partial}{\partial \theta} H = 0$. are set for the magnetic field. At the inside boundary of the ionosphere $R = I - \delta_u$ the magnetic field is considered unstimulated.

II. NUMERICAL MODELING METHOD

Discrete model of plasma. The idea of the "particle in a cell" method belongs to Harlow and has been used repeatedly for modeling not only laboratory (see, for example, [11-14]), but also cosmic plasma [10, 15-17]. This work utilizes the "CIC" ("clouds in a cell") method for computing the ion component of solar wind. The oncoming flow is approximated by a cold bundle of ions having spatial structure. Since equations of the field (1,2,6,7) are solved in planes $\varphi = 0, \pi/2$ (solution for $0 < \varphi < \pi/2$ is interpolated by trigonometric series), it has turned out to be expedient to inject plasma according to the following diagram, Figs. 2, 3. This initial distribution provides full approximation of parameters of plasma in sections $\varphi = 0, \pi/2$ with a minimal number of macroparticles $N = 100 \times 15 \times 7$. /7

Differential method of solving Maxwell's equations. In solving field equations, decomposition into Fourier series is utilized by φ:

$$H_r = h_{r2} \sin\varphi\,; \quad H_\theta = h_{\theta 2} \sin\varphi\,; \quad H_\varphi = h_{\varphi 2} \cos\varphi\,;$$

$$W_R = \frac{W_{R1} + W_{R2}}{2} + \cos 2\varphi \frac{W_{R1} - W_{R2}}{2}; \quad W_\theta = \frac{W_{\theta 1} + W_{\theta 2}}{2} + \cos 2\varphi$$

$$\ldots \frac{W_{\theta_1} - W_{\theta_2}}{2}; \quad W_y = W_{y_2} \sin\varphi; \quad E_x = \frac{E_{x_1} + E_{x_2}}{2} + \cos 2\varphi \frac{E_{x_1} - E_{x_2}}{2};$$

$$E_y = E_{y_2} \sin\varphi; \quad E_z = \frac{E_{z_1} + E_{z_2}}{2} + \cos 2\varphi \frac{E_{z_1} - E_{z_2}}{2};$$

$$n = \frac{n_1 + n_2}{2} + \cos 2\varphi \frac{n_1 - n_2}{2}.$$

u_1, u_2 -- value of field with $\varphi = 0$ and $\varphi = \pi/2$. The induction equation in planes $\varphi = 0$ and $\varphi = \pi/2$ is as follows:

$$\frac{\partial}{\partial t} h_i = L_1 h_i + L_2 h_i + f(h_j, \frac{\partial h_j}{\partial x_k}, \ldots),$$

$$L_1 h_i = W_k \frac{\partial}{\partial x_k} h_i + h_i \left(\frac{\partial}{\partial x_k} \alpha_k W_k + \beta_i\right), \qquad (9)$$

$$L_2 h_i = \frac{\partial}{\partial x_k} \left(\gamma_{kj} \frac{\partial}{\partial x_j} h_i\right); \quad h_i = \{h_r, h_\theta, h_\varphi\}.$$

In solving (9), a uniform grid according to R and θ (30 x 20), Fig. 4, is used. The Krapka-Nicholson method is used ($\sigma = 0{,}5$), differential operators L_1 and L_2 have the approximation $O(\Delta t)$ and $O(\Delta t^2)$, respectively. Mixed derivatives /8 are approximated by evident differentials.

Limitational conditions $h_r = \frac{\partial}{\partial \theta} h_\theta = 0, h_\varphi = h_\theta$. are placed at axis z for h_i.

In calculating the dynamics of ions and their concentration, grid II is introduced, shifted by $\Delta t/2$, $\Delta r/2$, $\Delta\theta/2$

relative to grid I, Fig. 4.

The equation of motion is approximated by a non-evident method with approximation $O\ (\Delta t^2)$.

III. RESULTS OF CALCULATIONS

Calculations are performed for the following parameters of oncoming flow:

$$M_a = M_s = 10;\ W_\infty/\omega_i R^* = 0{,}086;\ \varkappa = 5/3;$$
$$n_u = 10^2 - 10^4;\ Re_{mu} = 10^1 - 10^5;\ \delta_u = 0{,}1;$$
$$R_K = 1{,}35.$$

As a result of oncoming flow of plasma onto the ionosphere, electrons and ions penetrate to the depth of gyro-radius order $r_{i,e}$, since the electrical field in the ionosphere is small $E_u \ll H_u$.

Since with initial magnetic field, the dimensionless Larmor radius of ions $\frac{r_i}{R^*} = \frac{W_\infty}{\omega_i R^*} = 0.086$ is compared with the thickness of the ionosphere $\delta_u = 0.1$, ions, forming a current layer, fill up the ionosphere. Electrons having r_e 3 grades lower than r_i practically do not penetrate into the ionosphere. The final Larmor ion radius causes viscous interaction of plasma in the transitional sphere with the ionosphere. This fact significantly distinguishes this interaction model from gas-dynamic models [7-8]. 19

Let us consider in detail the flow picture in the regime $Re_{mu} = 10^3$, $n_u = 10^2$ at moment in time T = 0.85. Figures 5-6 give the distribution of solar wind plasma concentration in the

transitional sphere and the ionosphere in an equatorial and meridional plane. Evident from these graphs is a sharp increase in concentration directly behind the front of the shock wave. Away from the axis with $\theta \to \pi/2$, stimulation of concentration drops.

Figures 7-8 give the distribution of magnetic field module in an equatorial plane and the configuration of magnetic force lines in a meridianal plane. Directly behind the front of the shock wave, the magnetic field increases several times over, following the concentration. A condensation of force lines is observed near the ionopause, the plasma "frozen in" is disrupted and the magnetic field does not correspond to concentration. Final conductivity causes diffusions of the magnetic field into the ionosphere. The characteristic thickness of the "stagnant" sphere with strong magnetic field may be compared with the gyroradius in the transitional sphere.

Figures 9-10 give plasma current lines in the equatorial and meridianal planes. It is evident from the graphs that the current lines bend around the zone of the strong magnetic field. In spheres of relatively weak magnetic field, plasma flows into the ionopause, partially including the interplanetary field.

From calculation results, we can see the asymmetry in the flow picture in the equatorial and meridianal planes. Moreover, due to the influence of the final Larmor ion radius, a displacement of zero current line in the equatorial plane was observed.

Figure 11 gives the dependence of maximal strengthening of the magnetic field in the ionopause from Reynolds magnetic number in the ionosphere Re_{mu}. It is evident that with reduction of Re_{mu}, the diffusion of the magnetic field through /10

the ionosphere grows, and the "pumping" of the field in the ionopause is reduced. It should be noted that speed of convection in the ionosphere corresponding to effective diffusion may be evaluated as $V_u \sim \overline{Re}_{mu}^{-1}/\delta$ (δ -- characteristic diffusion scale).

Figure 12 gives the change in thickness of the transitional sphere in the subsolar point in time depending on Re_{mu}. Calculations have shown delay in formation of reflected particles and shock wave due to strong diffusion of the field in the ionosphere, and consequently a large Larmor ion radius. The thickness of the transitional sphere in our model exceeds the value of gasdynamic models [7-8]. This result is associated primarily with the rejection of the assumption that the ionopause is a tangential break, and consequently with increase of viscosity effects.

CONCLUSIONS

/11

1. During flow around the ionosphere, a considerable magnetic field is stimulated in the ionopause, associated with the final size of Larmor ion radius.

2. The amplitude of the magnetic field in the ionopause is significantly determined by the mechanism of "transfer" of the field through the ionosphere. Particularly, an accounting of real convection of the photoionosphere is necessary for evaluation of parameters of plasma and field in the ionopause.

3. The magnetic hydrodynamic boundary layer stimulated in the ionopause determines the flow in the transitional sphere.

4. Nonhydrodynamic approximation has additional asymmetry of flow relative to the meridional plane.

The author thanks A. A. Galeyev for his moral support and frequent fruitful discussions on this work.

REFERENCES

1. Sh. Sh. Dolginov, Ye. G. Yeroshenko, L. N. Zhuzgov. Kosmicheskiye issledovaniya ("Cosmic Research"), 1975, 13, 1, 108.

2. K. I. Gringauz, V. V. Bezrukikh, M. I. Verigin, A. P. Remizov. Kosmicheskiye issledovaniya ("Cosmic Research"), 1975, 13, 1, 123.

3. O. L. Vaysberg, A. V. Bogdanov, V. N. Smirnov, S. A. Romanov. Kosmicheskiye issledovaniya, 1975, 13, 1, 129.

4. O. L. Vaysberg, A. V. Bogdanov. Kosmicheskiye issledovaniya ("Cosmic Research"), 1974, 12, 2, 279.

5. Sh. Sh. Dolginov, Ye. G. Yeroshenko, L. N. Zhuzgov, et al. Letters to the Journal of Astronomy, 1976, 2, 1, 88.

6. K. I. Gringauz, V. V. Bezrukikh, T. K. Breus, et al. Letters to the Journal of Astronomy, 1976, 2, 2, 82.

7. O. M. Belotserkovskii and V. Ya. Mitnitskii. In the book: "Solar Wind Interaction with the Planets Mercury, Venus and Mars," Washington, NASA, 1976, SP-397, p. 121.

8. I. R. Spreiter. In the book: "Solar Wind Interaction with the Planets Mercury, Venus and Mars," Washington, NASA, 1976, SP-397, p. 135.

9. P. A. Cloutier. In the book: "Solar Wind Interaction with the Planets Mercury, Venus and Mars," Washington, NASA, 1976, SP-397, p. 111.

10. A. S. Lipatov. In the book: "Solar Wind Interaction with the Planets Mercury, Venus and Mars," Washington, NASA, 1976, SP-397, p. 151.

11. C. K. Birdsall, D. Fuss. J. Comput. Phys., 1969, 3, 1, 4.

12. Collected Works "Vychislitel'nyye metody v fizike plazmy" ("Computational Methods in the Physics of Plasma"), Moscow, Mir Press, 1974, pp. 321-345.

13. A. N. Polyudov, R. Z. Sagdeyev, Yu. S. Sigov. Preprint, Moscow, IPM AN SSSR, 1974, No. 128.

14. N. M. Zuyeva, V. S. Imshennik, O. V. Lokutsiyevskiy, M. S. Nikhaylova. Preprint No. 73, Moscow, IPM AN SSSR, 1975.

15. A. S. Lipatov. Preprint No. 196, Moscow, IKI AN SSSR.

16. A. S. Lipatov. Kosmicheskiye issledovaniya, 1976, 14, 3, 115.

17. K. Amano, T. Tsuda. J. Geomagnetism and Geoelectricity, 1977, 29, 1, 9.

FIGURE CAPTIONS

Fig. 1. Geometry of computational sphere of the problem

Fig. 2. Distribution of particles in planes X - Y

Fig. 3. Distribution of particles in planes X-Z, Y-Z

Fig. 4. Differential grids for computing field —x— and plasma parameters — .--

Fig. 5. Distribution of concentration in plane X-Z

Fig. 6. Distribution of concentration in plane Y-Z

Fig. 7. Lines of levels H in plane X-Z

Fig. 8. Magnetic field force lines in plane Y-Z

Fig. 9. Current lines in plane X-Z

Fig. 10. Current lines in plane Y-Z

Fig. 11. Dependence of value of magnetic field in the ionopause on Reynolds magnetic number ' the ionosphere

Fig. 12. Change in thickness of the transitional sphere through time for various Reynolds numbers of the ionosphere

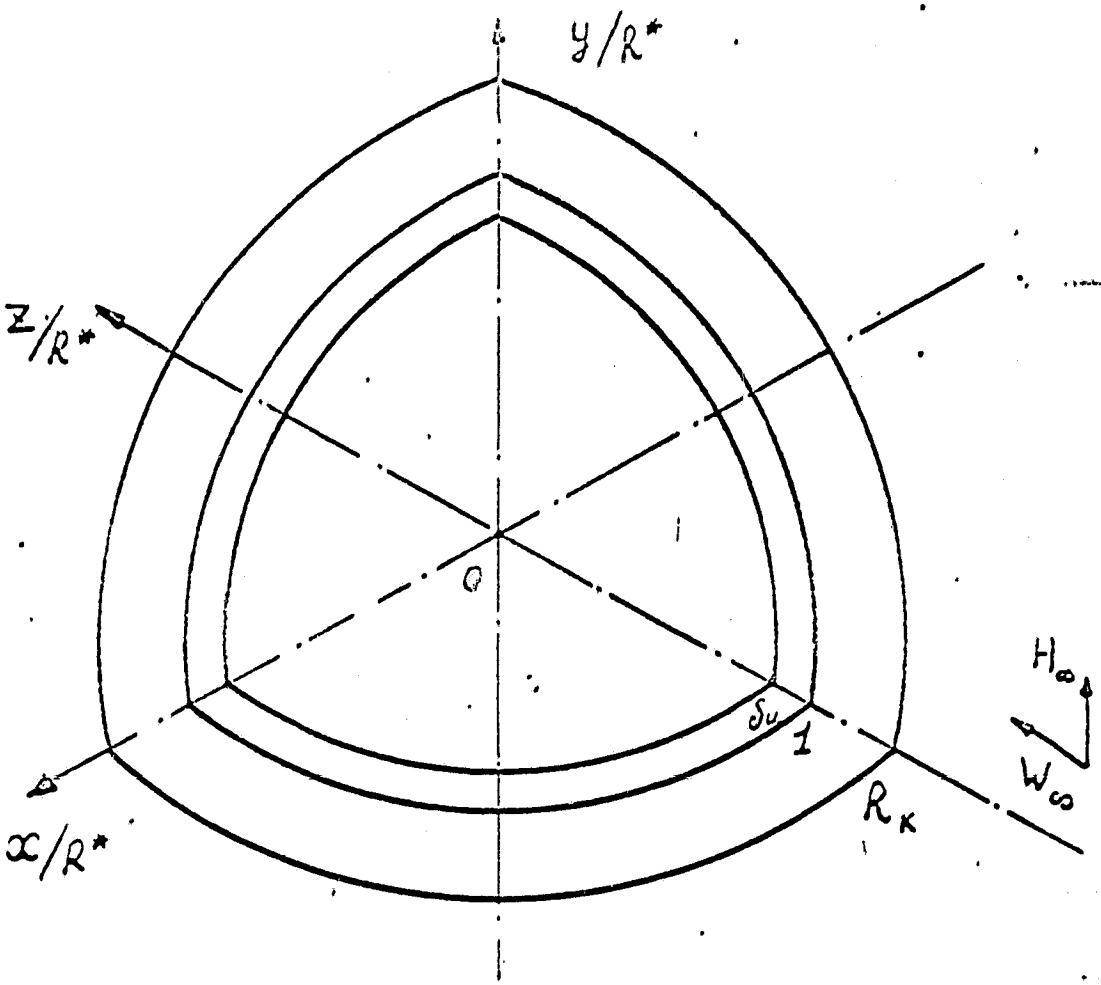

Fig. 1

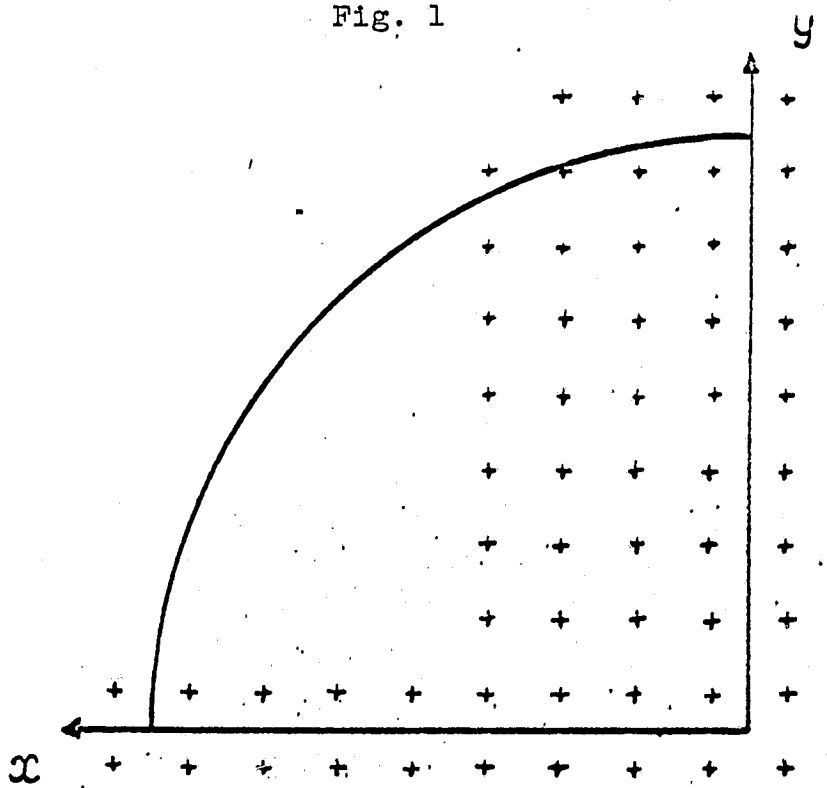

Fig. 2

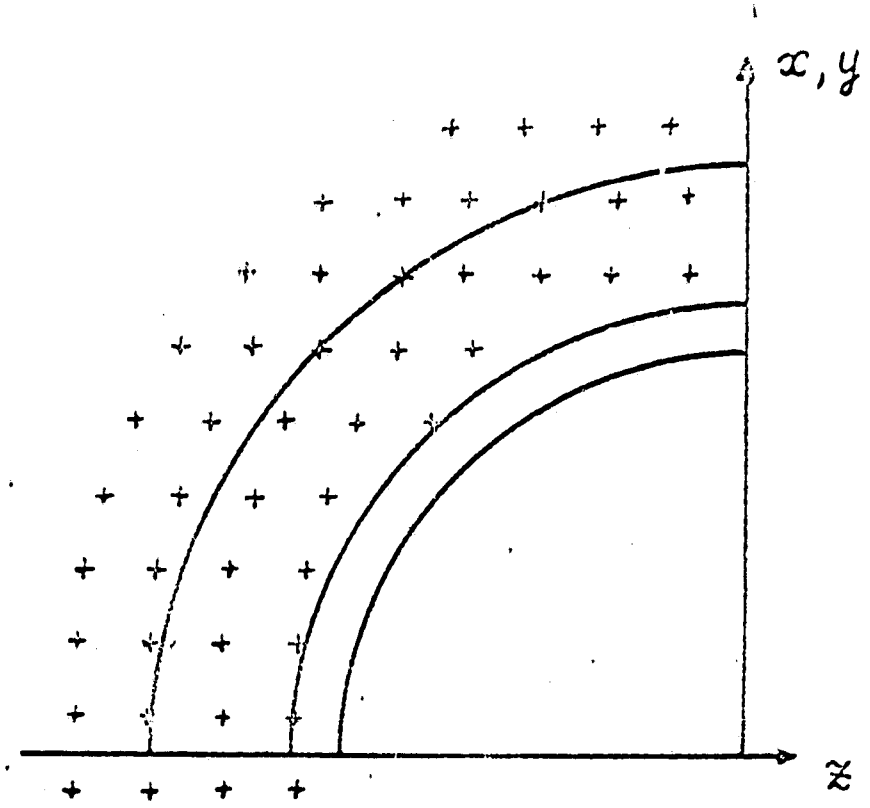

Fig. 3

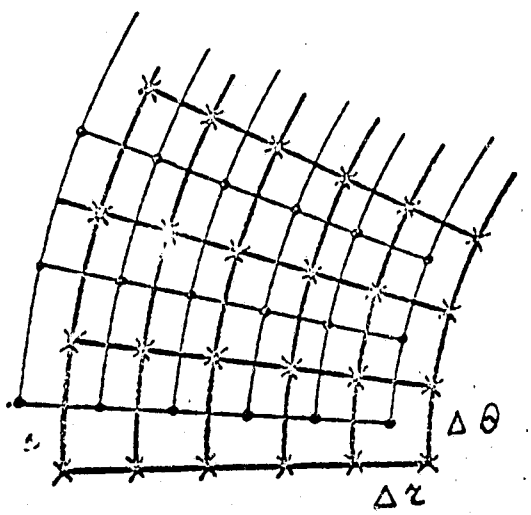

Fig. 4

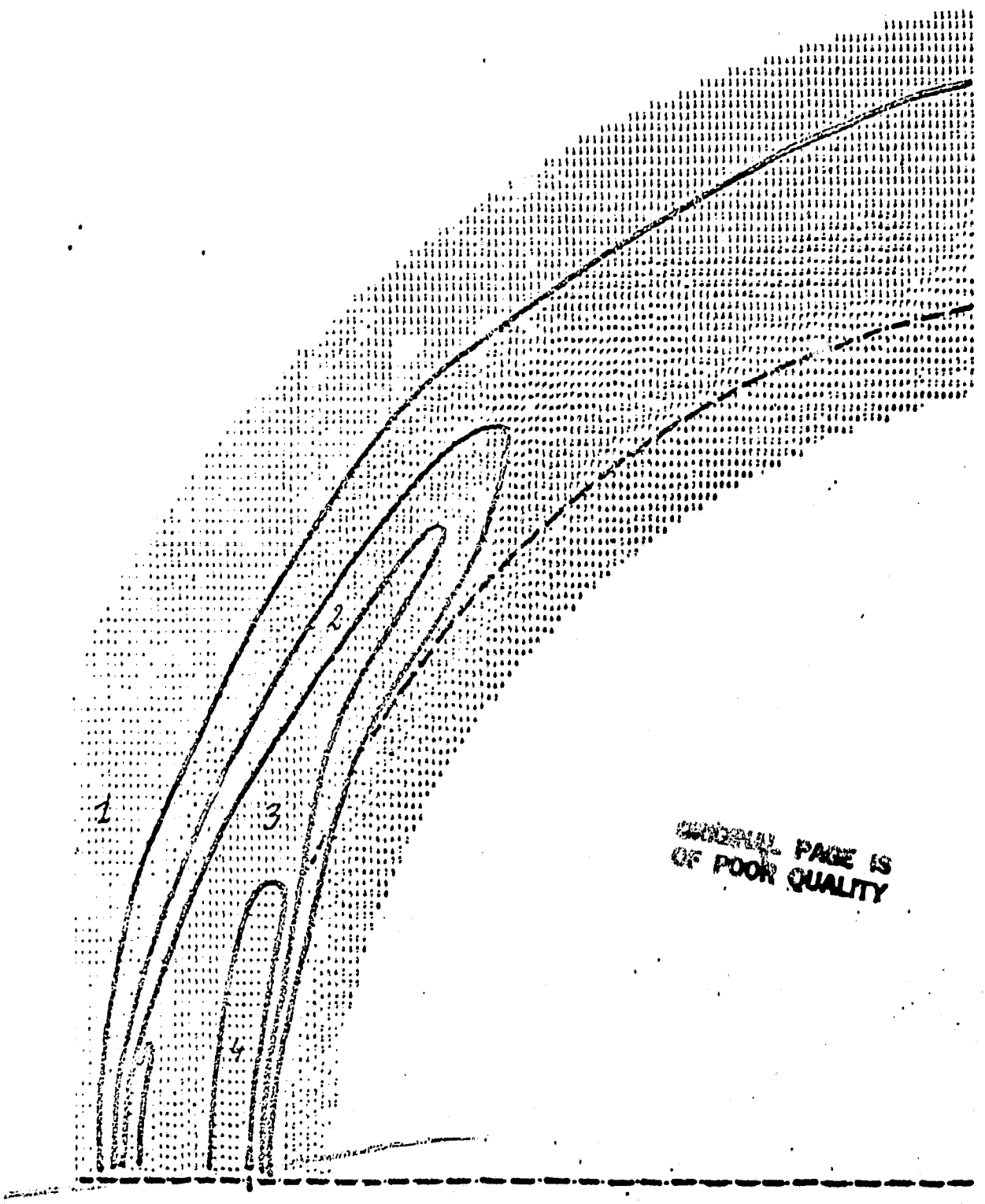

Fig. 5

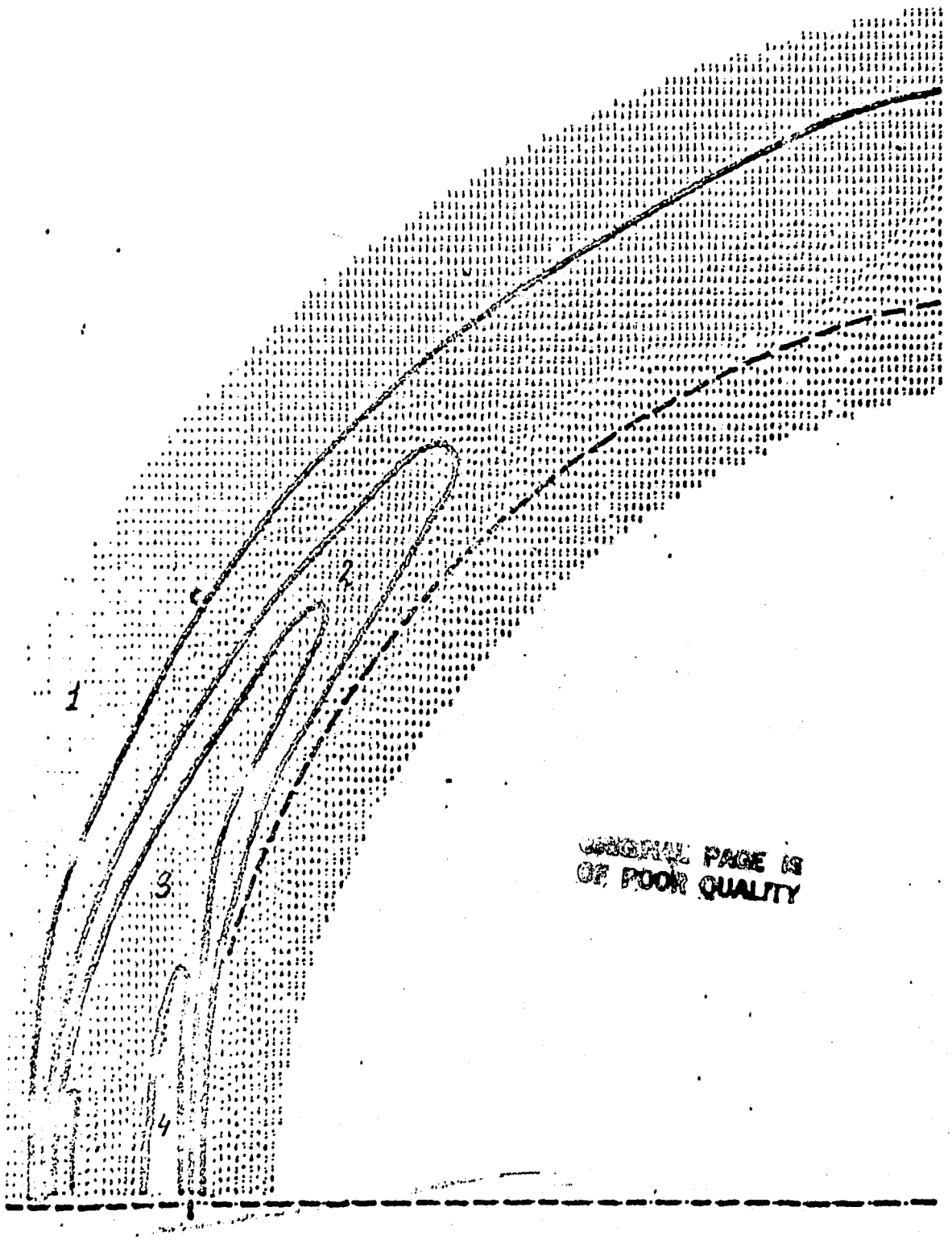

Fig. 6

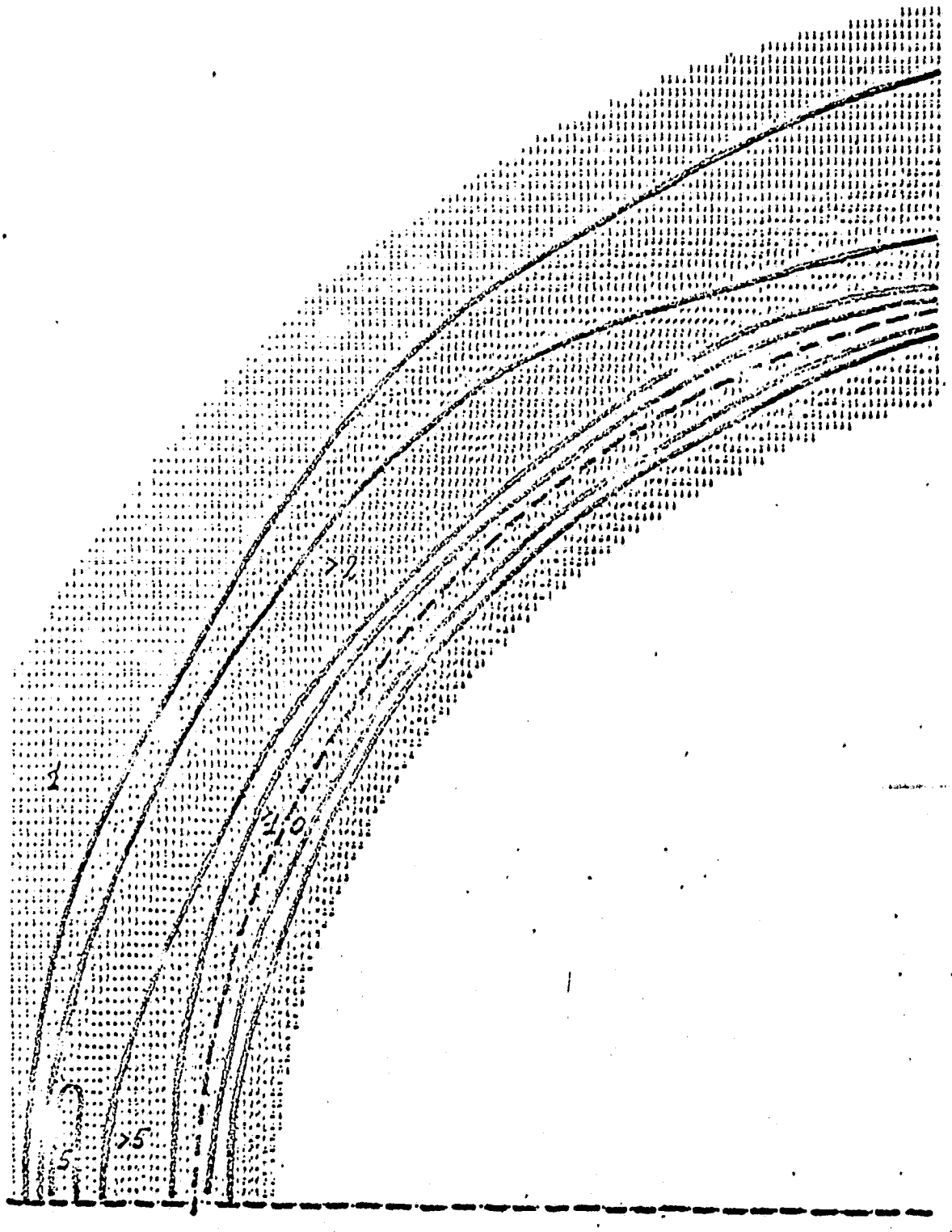

Fig. 7

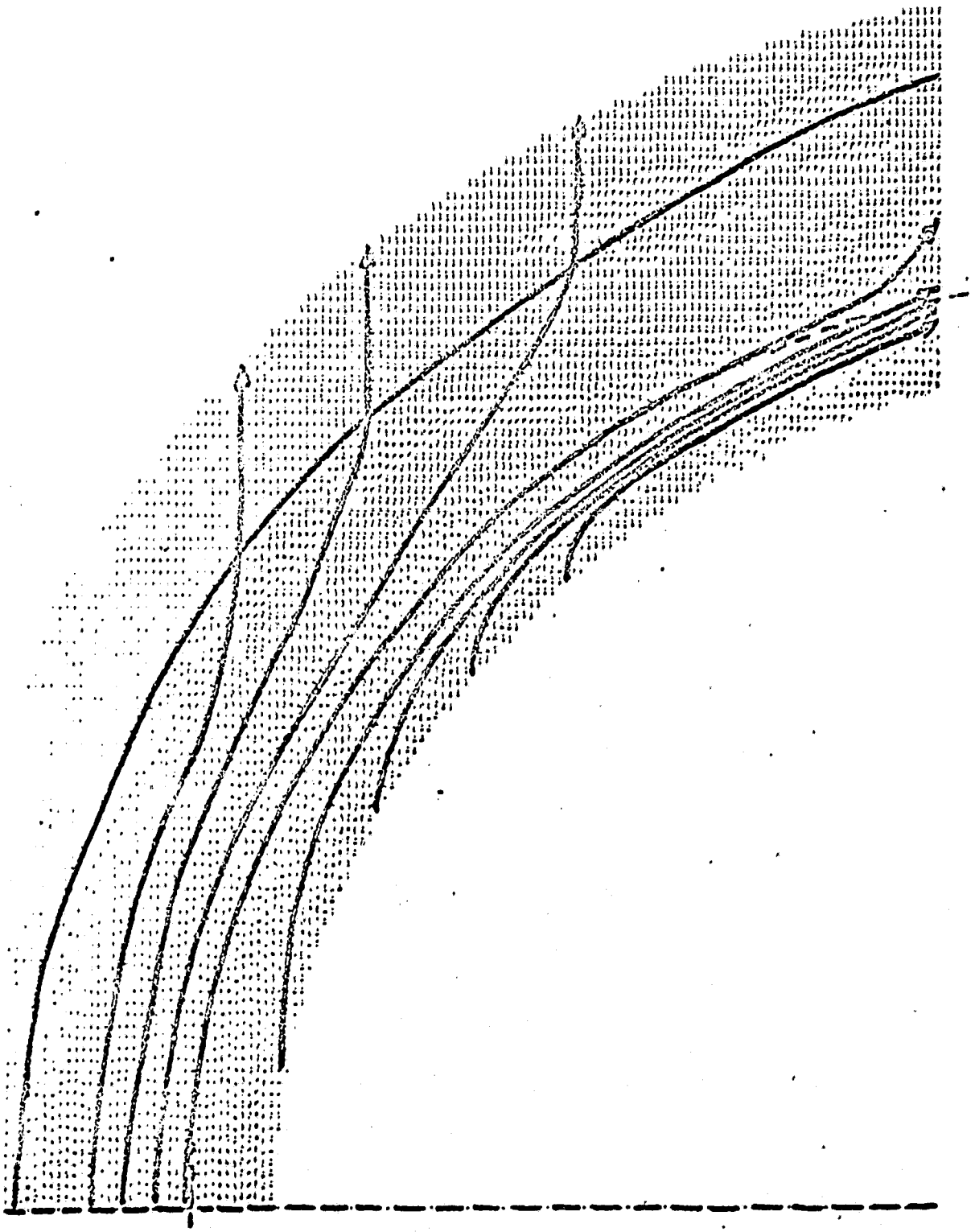

Fig. 8

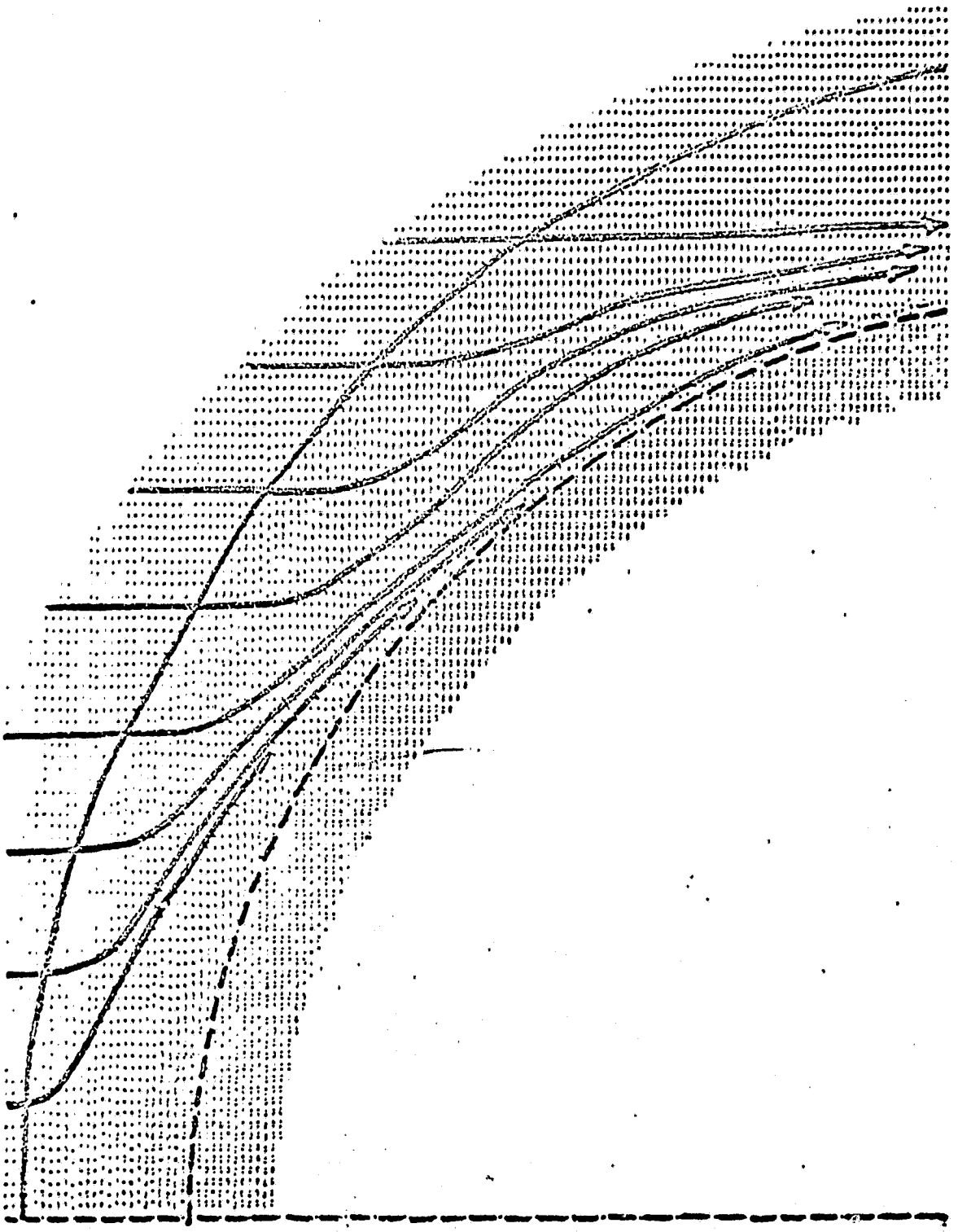

Fig. 9

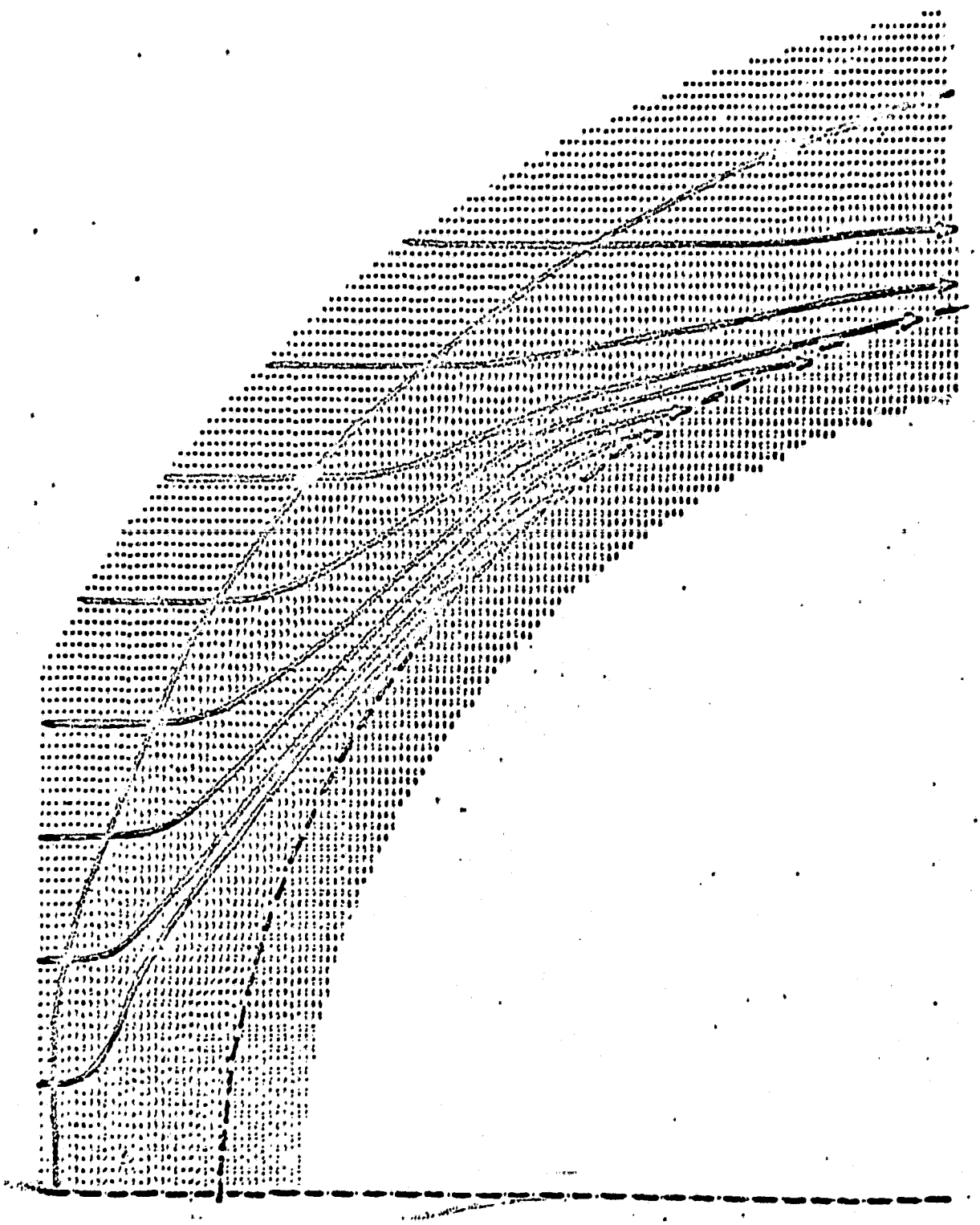

Fig. 10

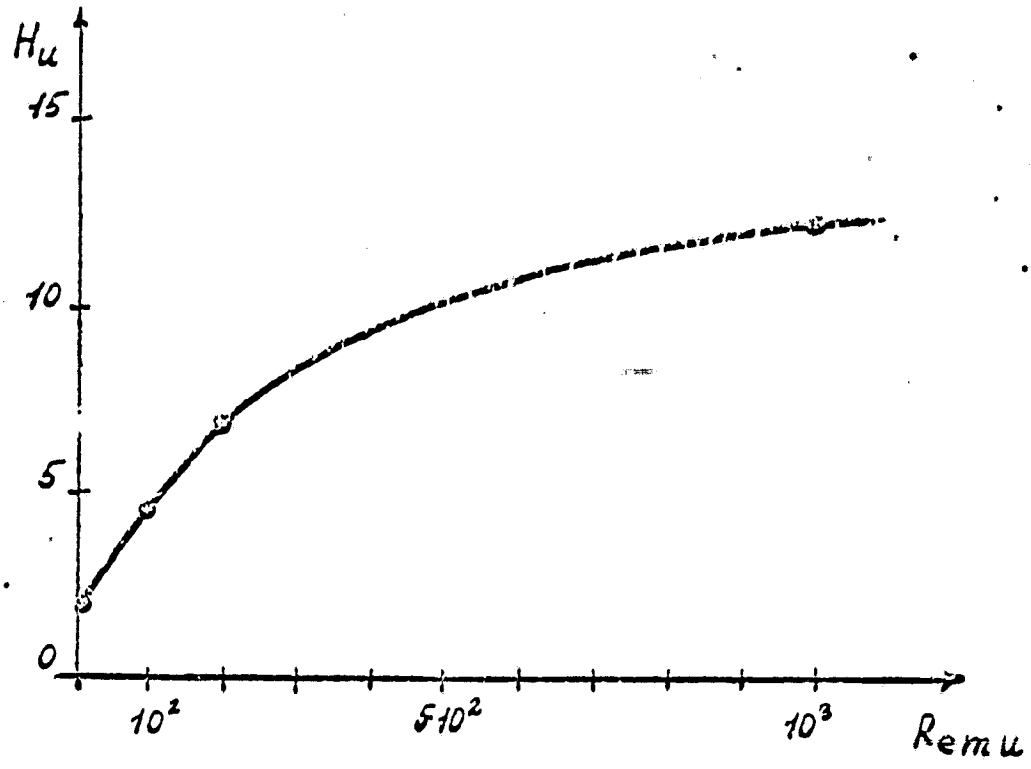
H_u
15
10
5
0
10^2
$5\cdot10^2$
10^3
Re_{mu}

Fig. 11

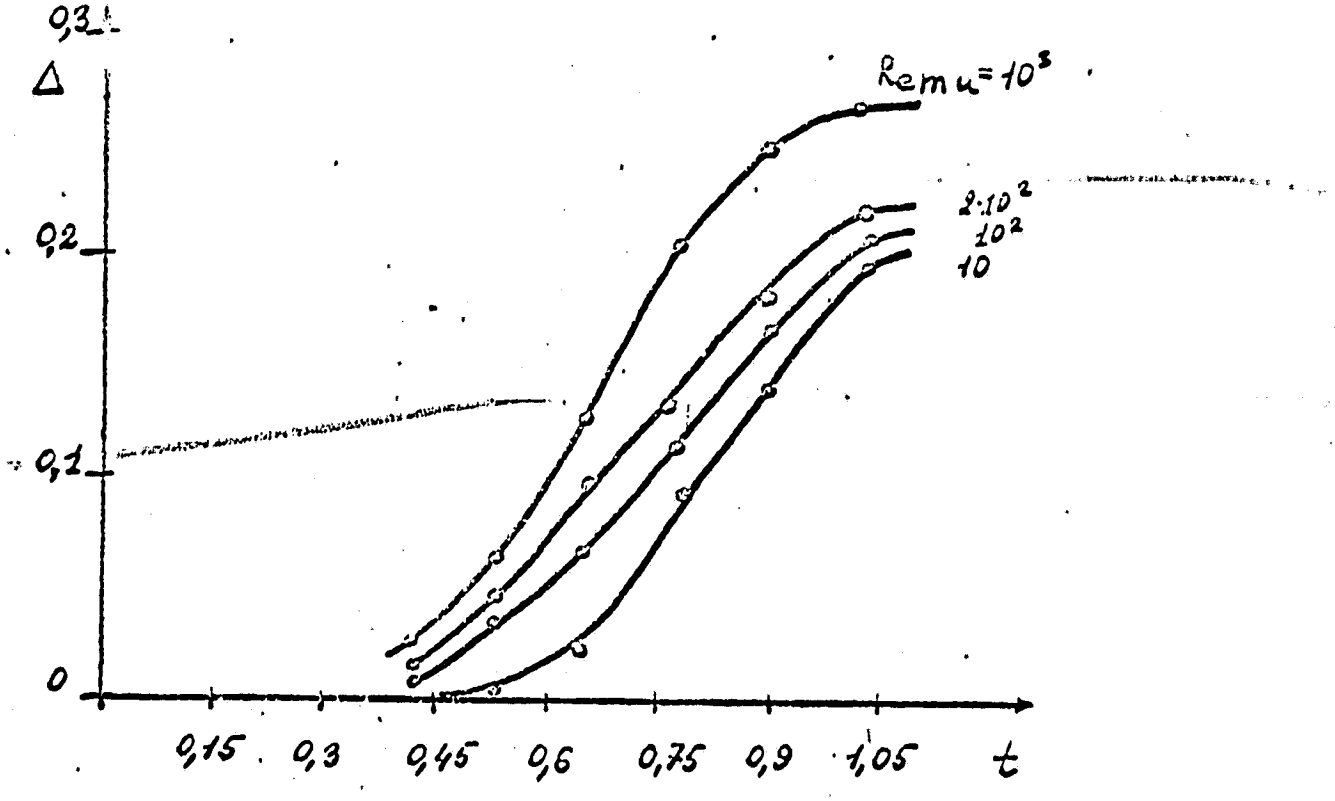
0,3
Δ
0,2
0,1
0
$Re_{mu}=10^3$
$2\cdot10^2$
10^2
10
0,15
0,3
0,45
0,6
0,75
0,9
1,05
t

Fig. 12